LOW-METALLICITY INHIBITION OF TYPE IA SUPERNOVAE
AND
GALACTIC AND COSMIC CHEMICAL EVOLUTION

Chiaki KOBAYASHI[1], Takuji TSUJIMOTO[2], Ken'ich NOMOTO[1], Izumi HACHISU[3], Mariko KATO[4]

[1] Department of Astronomy & Research Center for the Early Universe, School of Science, University of Tokyo,
Bunkyo-ku, Tokyo 113-0033, Japan; chiaki@astron.s.u-tokyo.ac.jp, nomoto@astron.s.u-tokyo.ac.jp
[2] National Astronomical Observatory, Mitaka, Tokyo 181-8588, Japan; tsuji@misty.mtk.nao.ac.jp
[3] Department of Earth Science and Astronomy, College of Arts and Sciences, University of Tokyo,
Meguro-ku, Tokyo 153-8902, Japan; hachisu@chianti.c.u-tokyo.ac.jp
[4] Department of Astronomy, Keio University, Kouhoku-ku, Yokohama 223-8521, Japan; mariko@educ.cc.keio.ac.jp

ABSTRACT

We introduce a metallicity dependence of Type Ia supernova (SN Ia) rate into the Galactic and cosmic chemical evolution models. In our SN Ia progenitor scenario, the accreting white dwarf (WD) blows a strong wind to reach the Chandrasekhar mass limit. If the iron abundance of the progenitors is as low as $[Fe/H] \lesssim -1$, then the wind is too weak for SNe Ia to occur. Our model successfully reproduces the observed chemical evolution in the solar neighborhood. We make the following predictions which can test this metallicity effect: 1) SNe Ia are not found in the low-iron abundance environments such as dwarf galaxies and the outskirts of spirals. 2) The cosmic SN Ia rate drops at $z \sim 1 - 2$ due to the low-iron abundance, which can be observed with the Next Generation Space Telescope. At $z \gtrsim 1 - 2$, SNe Ia can be found only in the environments where the timescale of metal enrichment is sufficiently short as in starburst galaxies and ellipticals.

The low-metallicity inhibition of SNe Ia can shed new light on the following issues: 1) The limited metallicity range of the SN Ia progenitors would imply that "evolution effects" are relatively small for the use of high redshift SNe Ia to determine the cosmological parameters. 2) WDs of halo populations are poor producers of SNe Ia, so that the WD contribution to the halo mass is not constrained from the iron abundance in the halo. 3) The abundance patterns of globular clusters and field stars in the Galactic halo lack of SN Ia signatures in spite of their age difference of several Gyrs, which can be explained by the low-metallicity inhibition of SNe Ia. 4) It could also explain why the SN Ia contamination is not seen in the damped Lyα systems for over a wide range of redshift.

Subject headings: Abundances — binaries: close — Cosmology: general — Galaxy: evolution — galaxies: evolution — stars: supernovae

1. INTRODUCTION

There exist two distinct types of supernova explosions: One is Type II supernovae (SNe II), which are the core collapse-induced explosions of short-lived massive stars ($\gtrsim 8M_\odot$) and produce more O and Mg relative to Fe (i.e., $[O/Fe] > 0$), and the other is Type Ia supernovae (SNe Ia), which are the thermonuclear explosions of accreting white dwarfs (WDs) in close binaries and produce mostly Fe and little O. The exact companion stars of the WDs have not been identified but must be relatively long-lived low mass stars.

The role of these two types of supernovae in the chemical evolution of galaxies can be seen in the abundance ratios of stars with different metallicities, most notably in the $[O/Fe]$-$[Fe/H]$ relation. Metal poor stars with $[Fe/H] \lesssim -1$ have $[O/Fe] \sim 0.45$ on the average (Nissen et al. 1994; Gratton 1991), while disk stars with $[Fe/H] \gtrsim -1$ show a decrease in $[O/Fe]$ with increasing metallicity (Edvardsson et al. 1993; Barbuy & Erdelyi-Mendes 1989; Gratton 1991). Such an evolutionary change in $[O/Fe]$ against $[Fe/H]$ has been explained with the early heavy element production by SNe II and the delayed enrichment of Fe by SNe Ia (Matteucci & Greggio 1986). Conversely, chemical evolution models can constrain the nature of still uncer-

tain progenitor systems of SNe Ia; for example, Yoshii, Tsujimoto, & Nomoto (1996) estimated the lifetime of SN Ia progenitors as long as $0.5 - 3$ Gyr.

SNe Ia have been discovered up to $z \sim 0.93$ by Supernova Cosmology Project (Perlmutter et al. 1997) and High-z Supernova Search Team (Garnavich et al. 1998). They have given the SN Ia rate at $z \sim 0.4$ (Pain et al. 1996) but will provide the SN Ia rate history over $0 < z < 1$. With the Next Generation Space Telescope, both SNe Ia and II will be observed through $z \sim 4$. In theoretical approach, the cosmic SN Ia rate as a function of redshift has been constructed for a cosmic star formation rate (SFR) (Ruiz-Lapuente & Canal 1998; Yungelson & Livio 1998; Sadat et al. 1998; Madau, Valle & Panagia 1998). The comparison between the model prediction and observations can constrain the lifetime of the progenitor systems of SNe Ia.

The progenitors of the majority of SNe Ia are most likely the Chandrasekhar (Ch) mass WDs (e.g., Nomoto, Iwamoto & Kishimoto 1997a for a recent review), although the sub-Ch mass models might correspond to some peculiar sub-luminous SNe Ia. The early time spectra of the majority of SNe Ia are in excellent agreement with the synthetic spectra of the Ch mass models, while the spectra of the sub-Ch mass models are too blue to be compatible

with observations (Höflich & Khokhlov 1996; Nugent et al. 1997). For the evolution of accreting WDs toward the Ch mass, two scenarios have been proposed: One is a double degenerate (DD) scenario, i.e., merging of double C+O WDs with a combined mass surpassing the Ch mass limit (Iben & Tutukov 1984; Webbink 1984), and the other is a single degenerate (SD) scenario, i.e., accretion of hydrogen-rich matter via mass transfer from a binary companion (e.g., Nomoto et al. 1994 for a review). The issue of DD vs. SD is still debated (e.g., Branch et al. 1995 for a review), although theoretical modeling has indicated that the merging of WDs does not make typical SNe Ia (Saio & Nomoto 1985, 1998).

For the SD scenario, a new evolutionary model has been proposed by Hachisu, Kato, & Nomoto (1996, 1998; hereafter HKN96 and HKN98, respectively) and Hachisu & Kato (1998; hereafter HK98). HKN96 have shown that if the accretion rate exceeds a certain limit, the WD blows a strong wind and burns hydrogen steadily to increase the WD mass (see section 2). HKN98 have further invoked the effect of stripping-off of the envelope from the companion by the strong wind, and shown that the WD can reach the Ch mass for much wider binary parameter space than found by HKN96, Li & van den Heuvel (1997), and Yungelson & Livio (1998); the allowed parameter space may be large enough to account for the SN Ia frequency. Moreover, HK98 have found an important metallicity effect; if the iron abundance of the accreted matter is as low as $[Fe/H] \lesssim -1$, the WD wind is too weak to increase the WD mass through the Ch mass.

In the present *Letter*, we apply the above two scenarios to the chemical evolution models, and compare the cases with and without the metallicity effect on SNe Ia. We have found that the model for SD scenario with the metallicity effect is significantly better to reproduce the evolutionary change in [O/Fe] and other properties (Section 3). Using the metallicity dependent SN Ia rate, we make a prediction for the cosmic supernova rate history (Section 4). In section 5 we discuss other implications on the Galactic halo objects, damped Lyα (DLA) systems and cosmology.

2. TYPE IA SUPERNOVA PROGENITOR SYSTEM

Our SD scenario has two progenitor systems: One is a red-giant (RG) companion with the initial mass of $M_{RG,0} \sim 1M_\odot$ and the orbital period of tens to hundreds days (HKN96; HKN98). The other is a near main-sequence (MS) companion with the initial mass of $M_{MS,0} \sim 2-3M_\odot$ and the period of several tenths of a day to several days (Li & van den Heuvel 1997; HKN98). In these SD scenarios, optically thick winds from the mass accreting WD play an essential role in stabilizing the mass transfer and escaping from forming a common envelope. The optically thick winds are driven by a strong peak of OPAL opacity at $\log T(K) \sim 5.2$ (e.g., Iglesias & Rogers 1993). Since the peak is due to iron lines, the optically thick winds depend strongly on the metallicity (HK98).

Figure 1 shows the metallicity dependence of the optically thick winds. The strong winds are possible only for the region above the dashed line. The term "weak" implies that the wind velocity at the photosphere does not exceed the escape velocity there, that is, it cannot blow the accreted matter off the WD. For the metallicity as small as $Z = 0.001$, the opacity peak at $\log T \sim 5.2$ is very weak, being smaller than the peak of helium lines at $\log T \sim 4.6$. Then, the wind is driven by the helium line peak rather than the iron line peak, which we call "He wind" instead of "Fe wind". Since only the initial WD mass of $M_{WD,0} \leq 1.2M_\odot$ can produce an SN Ia (Nomoto & Kondo 1991), SN Ia events occur only for the progenitors with $[Fe/H] \gtrsim -1.1$, which is adopted in our chemical evolution model.

Figure 2 shows the SN Ia regions in the diagram of the initial orbital period vs. the initial mass of the companion star for the initial WD mass of $M_{WD,0} = 1.0M_\odot$ (see HK98 for other $M_{WD,0}$). In these regions, the accretion from the companion star increases the WD mass successfully through the occurrence of SN Ia. The dashed line shows the case of solar abundance ($Z = 0.02$), while the solid line shows the much lower metallicity case of $Z = 0.004$. The size of these regions clearly demonstrate the metallicity effect, i.e., SN Ia regions are much smaller for smaller metallicity. The initial mass ranges of the companion stars for $Z = 0.004$ are $0.9M_\odot \lesssim M_{RG,0} \lesssim 1.5M_\odot$ for the WD+RG system and $1.8M_\odot \lesssim M_{MS,0} \lesssim 2.6M_\odot$ for the WD+MS system.

3. THE CHEMICAL EVOLUTION IN THE SOLAR NEIGHBORHOOD

We use the chemical evolution model which allows the material infall from outside the disk region. For the infall rate, we adopt a formula which is proportional to $t \exp[-t/\tau]$ with a infall timescale of $\tau = 5$ Gyr (Yoshii et al. 1996). The Galactic age is assumed to be 15 Gyr. The SFR is assumed to be proportional to the gas fraction with a constant rate coefficient of 0.37 Gyr^{-1}. For the initial mass function (IMF), we assume a power-law mass spectrum with a Salpeter slope of $x = 1.35$ in the range of $0.05M_\odot \leq M \leq 50M_\odot$ (Tsujimoto et al. 1997). We take the nucleosynthesis yields of SNe Ia and II from Tsujimoto et al. (1995; see Nomoto et al. 1997b,c for details) and the metallicity dependent main-sequence lifetime from Kodama (1997).

For the SD scenario, the lifetime of SNe Ia is determined from the main-sequence lifetime of the companion star. We adopt the initial mass ranges of the binary companion stars obtained in section 2. The distribution function of the initial mass of the companions is taken from the mass ratio distribution in binaries (Duguennoy & Mayor 1991), which is approximated by a power-law mass spectrum with a slope $x = 0.35$. The fraction of primary stars of $3-8M_\odot$ which eventually produce SNe Ia is set to be 0.04 for both the WD+MS and the WD+RG systems, adjusted to reproduce the chemical evolution in the solar neighborhood. For the DD scenario we adopt the distribution function of the lifetime of SNe Ia by Tutukov & Yungelson (1994), majority of which is $\sim 0.1-0.3$ Gyr.

Figure 3 shows the evolutionary change in [O/Fe] for three SN Ia models. The dotted line is for the DD scenario. The other lines are for our SD scenario with (solid line) and without (dashed line) the metallicity effect on SNe Ia. The results are as follows.

- In the DD scenario the lifetime of the majority of SNe Ia is shorter than 0.3 Gyr. Then the decrease in

[O/Fe] starts at [Fe/H] ~ -2, which is too early compared with the observed decrease in [O/Fe] starting at [Fe/H] ~ -1.

- For the SD scenario with no metallicity effect, the companion star with $M \sim 2.6 M_\odot$ evolves off the main-sequence to give rise to SNe Ia at the age of ~ 0.6 Gyr. The resultant decrease in [O/Fe] starts too early to be compatible with the observations.

- For the metallicity dependent SD scenario, SNe Ia occur at [Fe/H] $\gtrsim -1$, which naturally reproduce the observed break in [O/Fe] at [Fe/H] ~ -1.

We also perform the Kolmogorov-Smirnov (KS) test to estimate how well the predicted abundance patterns agree with the observed one (Edvardsson et al. 1993), and tabulate the resultant probabilities in Table 1. The KS test is applied to the abundance distribution function in the range of $-1.15 \le$ [Fe/H] ≤ 0.45 and to the evolutionary behavior of [O/Fe] in the range of $-0.85 \le$ [Fe/H] ≤ 0.02. The predicted abundance distribution functions are identical with the observational data with more than 84% probability for both the DD and SD scenarios. For our SN Ia model with the metallicity effect, the calculated [O/Fe] against [Fe/H] fits well to the observations with 85% probability. But when we neglect the metallicity effect, the probability decreases to 57%. For the DD scenario the calculated [O/Fe] is rejected with 82% probability.

4. COSMIC SUPERNOVA RATE

We apply our SN Ia progenitor scenario to predict the cosmic supernova rate history and the cosmic chemical evolution corresponding to the observed cosmic SFR (Madau et al. 1996; Connolly et al. 1997). The photometric evolution is calculated with the spectral synthesis population database taken from Kodama (1997). We adopt $H_0 = 50$ km s^{-1} Mpc^{-1}, $\Omega_0 = 0.2$, $\lambda_0 = 0$, and the redshift at the formation epoch of galaxies $z_f = 5$. We use the initial comoving density of gas $\Omega_{g\infty} = 2 \times 10^{-3}$ (Pei & Fall 1995).

Figure 4 shows the cosmic supernova rate per $10^{10} L_\odot$ per century (SNu). The long dashed line is for SNe II and the other lines for SNe Ia with (solid line) and without (dashed line) the metallicity effect. If we do not include the metallicity effect, the SN Ia rate is almost flat from the present to higher redshift, and decreases toward the formation epoch of galaxies. If we include the metallicity effect, the SN Ia rate drops at $z \sim 1.2$, where the iron abundance of the gas in the universe is too low (i.e., [Fe/H] $\lesssim -1$) for the progenitors of SNe Ia to make explosions. The redshift where the SN Ia rate drops is determined by the speed of the chemical enrichment, which depends on the effect of dust extinction on the cosmic SFR (Pettini et al. 1997), cosmology, galaxy formation epoch and the initial gas density. Taking into account these uncertainties, the break in the SN Ia rate occurs at $z = 1 - 2$. We should note that galaxies being responsible for the global SFR have different heavy-element enrichment timescale, some of which are starburst galaxies and ellipticals achieving [Fe/H] ~ -1 in much shorter timescale than in Figure 4. In such galaxies SNe Ia can occur even at $z \gtrsim 1 - 2$.

5. CONCLUSIONS AND DISCUSSION

We introduce a metallicity dependence of the SN Ia rate in the Galactic and cosmic chemical evolution models. In our scenario involving a strong wind from WDs, little SNe Ia occur at [Fe/H] $\lesssim -1$. Our model successfully reproduces the observed chemical evolution in the solar neighborhood. We make the following predictions which can test this metallicity effect. 1) SNe Ia are not found in the low-iron abundance environments such as dwarf galaxies and the outskirts of spirals. 2) The cosmic SN Ia rate drops at $z \sim 1 - 2$ due to the low-iron abundance, which can be observed with the Next Generation Space Telescope. At $z \gtrsim 1 - 2$, SNe Ia can be found only in the environments where the timescale of metal enrichment is sufficiently short as in starburst galaxies and ellipticals.

The low-metallicity inhibition of SNe Ia can shed new light on the following issues:

1) It imposes a limit on the metallicity range of the SN Ia progenitors. This would imply that "evolution effects" are relatively small for the use of high redshift SNe Ia to determine the cosmological parameters.

2) Microlensing experiments (Alcock et al. 1997) suggest the WD-dominated Galactic halo. The existence of so many WDs results in too much iron enrichment from SNe Ia (Canal, Isern & Ruiz-Lapuente 1997). However, WDs of halo populations are poor producers of SNe Ia, so that the iron abundance of the halo may not put the strong constraint on the contribution of WDs. Note, however, that there exist several other arguments against the WD-dominated halo (e.g., Charlot & Silk 1995; Gibson & Mould 1997).

3) The Galactic halo is a low-metallicity system with [Fe/H] $\lesssim -1$ and have an abundance pattern of genuine SN II origin, i.e., the overabundances of α-elements relative to Fe as [α/Fe] > 0 (e.g., Wheeler, Sneden & Truran 1989). However there exist age differences of several Gyrs among the clusters (Chaboyer, Demarque & Sarajedini 1996) as well as field stars (Schuster & Nissen 1989). Since the shortest lifetime of SNe Ia is ~ 0.6 Gyr for the MS+WD close binary systems, SN Ia contamination would be seen in [α/Fe] if there were no metallicity effect on SNe Ia. This apparent discrepancy between the age difference and the high [α/Fe] can be resolved by the low-metallicity inhibition of SNe Ia.

4) Similar interpretation holds also for DLA systems. The DLA systems observed at $0.7 < z < 4.4$ have [Fe/H]= -2.5 to -1 and indicate [α/Fe] > 0 (Lu et al. 1996). Lu et al. (1996) suggested there may exist the age-metallicity relation in DLA systems, which implies that DLA systems grown through a common chemical history spanning over several Gyrs. If so, the SN II-like abundance pattern in DLA systems needs the introduction of the metallicity dependent SN Ia rate to avoid the contamination of SN Ia products.

spectra, and David Branch for many useful comments to improve the paper.

REFERENCES

Alcock, C., et al. 1997, ApJ, 486, 697
Barbuy, B., & Erdelyi-Mendes, M. 1989, A&A, 214, 239
Branch, D., Livio, M., Yungelson, L. R., Boffi, F. R., & Baron, E. 1995, PASP, 107, 717
Chaboyer, B., Demarque, P., & Sarajedini, A. 1996, ApJ, 459, 558
Charlot, S., & Silk, J. 1995, ApJ, 445, 124
Canal, R., Isern, J., & Ruiz-Lapuente, P. 1997, ApJ, 488, L35
Connolly, A. J., Szalay, A. S., Dickinson, M., SubbaRao, M. U., & Brunner, R. J. 1997, ApJ, 486, L11
Duguennoy, A., & Mayor, M. 1991, A&A, 248, 485
Edvardsson, B., Andersen, J., Gustafsson, B., Lambert, D. L., Nissen, P. E., & Tomkin, J. 1993, A&A, 275, 101
Garnavich, P., et al. 1998, ApJ, 493, 53
Gibson, B. K., & Mould, J. R. 1997, ApJ, 482, 98
Gratton, R. G. 1991, in IAU Symp. 145, Evolution of Stars: The Photometric Abundance Connection, ed. G. Michaud & A. V. Tutukov (Montreal: Univ. Montreal), 27
Hachisu, I., & Kato, M., 1998, in preparation (HK98)
Hachisu, I., Kato, M., & Nomoto, K. 1996, ApJ, 470, L97 (HKN96)
Hachisu, I., Kato, M., & Nomoto, K. 1998, preprint to be submitted to ApJ(HKN98)
Höflich, P., & Khokhlov, A. 1996, ApJ, 457, 500
Iben, I. Jr., & Tutukov, A. V. 1984, ApJS, 54, 335
Iglesias, C. A., & Rogers, F. 1993, ApJ, 412, 752
Kodama, T. 1997, Ph.D. Thesis. University of Tokyo
Li, X. -D., & van den Heuvel, E. P. J. 1997, A&A, 322, L9
Lu, L., Sargent, W. L. W., Barlow, T. A., Churchill, C. W., & Vogt, S. S. 1996, ApJS, 107, 475
Madau, P., Ferguson, H. C., Dickinson, M. E., Giavalisco, M., Steidel, C. C., & Fruchter, A. 1996, MNRAS, 283, 1388
Madau, P., Valle, D. M., & Panagia, N. 1998, MNRAS, in press (astro-ph/980328)
Matteucci, F., & Greggio, L. 1986, A&A, 154, 279

Nissen, P. E., Gustafsson, B., Edvardsson, B., & Gilmore, G. 1994, A&A, 285, 440
Nomoto, K., & Kondo, Y. 1991, ApJ, 367, L19
Nomoto, K., Iwamoto, K., & Kishimoto, N. 1997a, Science, 276, 1378
Nomoto, K., et al. 1997b, Nuclear Physics, A616, 79c
Nomoto, K., et al. 1997c, Nuclear Physics, A621, 467c
Nomoto, K., Yamaoka, H., Shigeyama, T., Kumagai, S., & Tsujimoto, T. 1994, in Supernovae, Les Houches Session LIV, ed. S.A. Bludman et al. (Amsterdam: North-Holland), 199
Nugent, P., Baron, E., Branch, D., Fisher, A., & Hauschildt, P. H. 1997, ApJ, 485, 812
Pain, R., et al. 1996, ApJ, 473, 356
Pei, Y. C., & Fall, S. M., 1995, ApJ, 454, 69
Perlmutter, S., et al. 1997, ApJ, 483, 565
Pettini, M., Steidel, C. C., Dickinson, M., Kellogg, M., Giavalisco, M., & Adelberger, K. L, 1997, in The Ultraviolet Universe at Low and High Redshift, ed. W. Waller, (Woodbury: AIP Press), in press
Ruiz-Lapuente, P., & Canal, R. 1998, ApJ, 497, L57
Sadat, R., Blanchard, A., Guiderdoni, B., & Silk, J. 1998, A&A, 331, L69
Saio, H., & Nomoto, K. 1985, A&A, 150, L21
Saio, H., & Nomoto, K. 1998, ApJ, 500, 388
Schuster, W. J., & Nissen, P. E. 1989, A&A, 222, 69
Tsujimoto, T., Nomoto, K., Yoshii, Y., Hashimoto, M., Yanagida, S., & Thielemann, F.-K. 1995, MNRAS, 277, 945
Tsujimoto, T., Yoshii, Y., Nomoto, K., Matteucci, F., Thielemann, F. -K., & Hashimoto, M. 1997, ApJ, 483, 228
Tutukov, A. V., & Yungelson, L. R. 1994, MNRAS, 268, 871
Webbink, R. F. 1984, ApJ, 277, 355
Wheeler, J. C., Sneden, C., & Truran, J. W. 1989, ARA&A, 27, 279
Yoshii, Y., Tsujimoto, T., & Nomoto, K. 1996, ApJ, 462, 266
Yungelson, L., & Livio, M. 1998, ApJ, 497, 168

TABLE 1

PROBABILITIES GIVEN BY THE KOLMOGOROV-SMIRNOV TEST

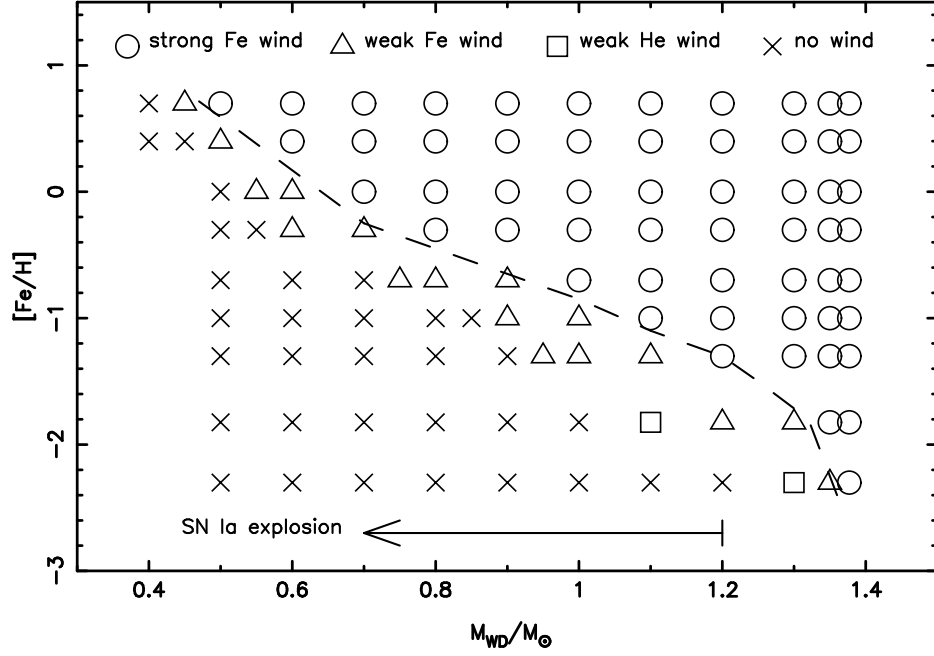| SN Ia progenitor model	Probability	
	abundance ratio	abundance distribution
SD with the metallicity effect	85.0 %	89.5 %
SD without the metallicity effect	57.2 %	84.8 %
DD scenario	17.6 %	86.9 %

FIG. 1.— Metallicity dependence of optically thick winds is shown in WD mass vs. metallicity diagram. We regard the wind as "strong" if the wind velocity at the photosphere exceeds the escape velocity but "weak" if the wind velocity is lower than the escape velocity. The term of "He" or "Fe" wind denotes that the wind is accelerated by the peak of iron lines near $\log T(\mathrm{K}) \sim 5.2$ or of helium lines near $\log T(\mathrm{K}) \sim 4.6$. The dashed line indicates the demarcation between the "strong" wind and the "weak" wind.
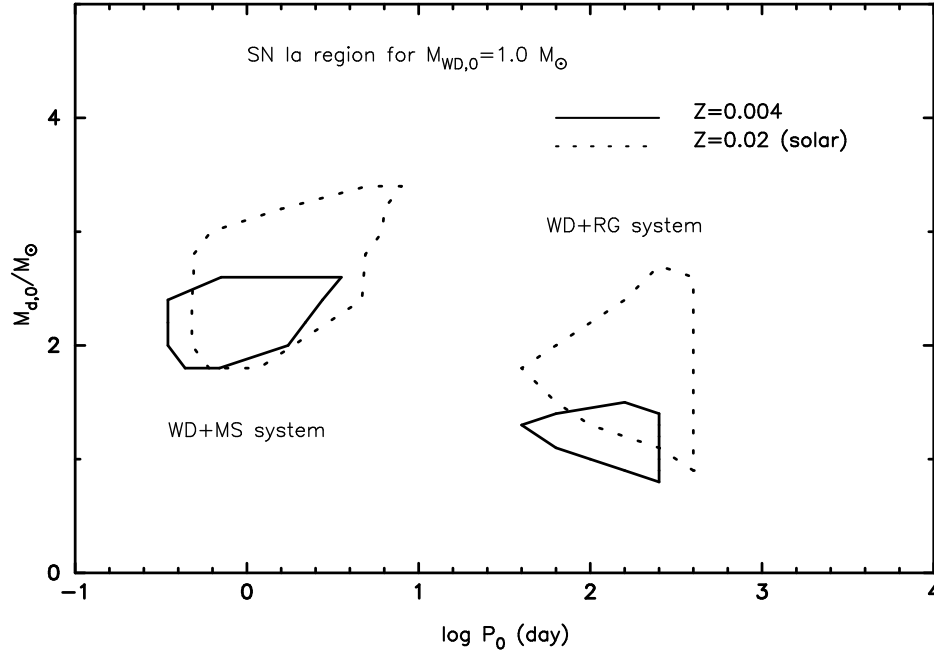

FIG. 2.— The regions of SNe Ia is plotted in the initial orbital period vs. the initial companion mass diagram for the initial WD mass of $M_{\mathrm{WD},0} = 1.0 M_\odot$. The dashed and solid lines represent the cases of solar abundance ($Z = 0.02$) and much lower metallicity of $Z = 0.004$, respectively. The left and the right regions correspond to the WD+MS and the WD+RG systems, respectively.
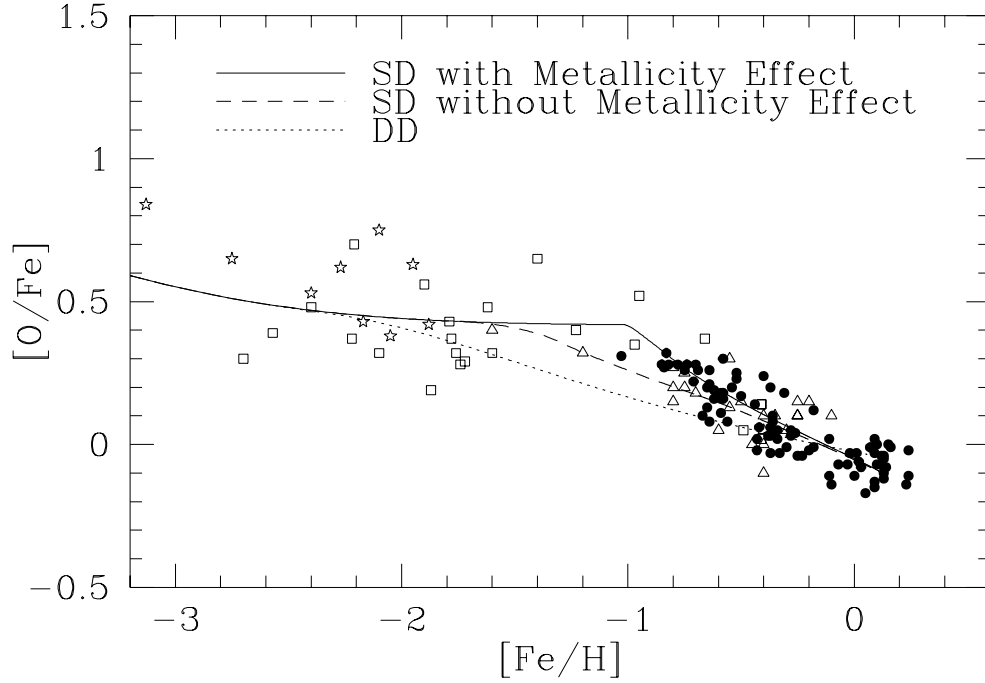
FIG. 3.— The evolutionary change in [O/Fe] against [Fe/H] for three SN Ia models. The dotted line is for the DD scenario where SNe Ia occur by merging of two WDs at a rate given by Tutukov & Yungelson (1994). The other lines are for our SD scenario with (solid line) and without (dashed line) the metallicity effect on SNe Ia. Observational data sources: filled circles, Edvardsson et al. (1993); open triangles, Barbuy & Erdelyi-Mendes (1989); stars, Nissen et al. (1994); open squares, Gratton (1991).
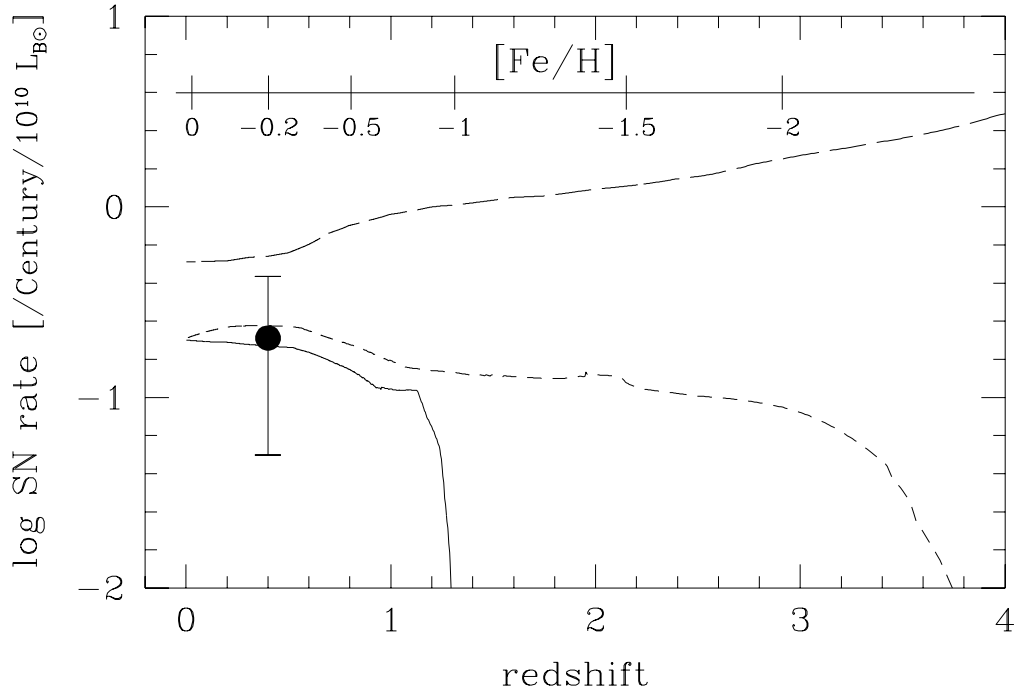

FIG. 4.— The cosmic supernova rate per $10^{10}L_\odot$ per century (SNu). The long-dashed line is for SNe II and the other lines for SNe Ia with (solid line) and without (dashed line) the metallicity effect. The filled circle is the observed SN Ia rate at $z \sim 0.4$ (Pain et al. 1996). The iron-abundance scale in the abscissa is calculated with the metallicity effect on SNe Ia.